Int. J. Electrochem. Sci., 10 **(2015)** 7941 - 7954

International Journal of
ELECTROCHEMICAL
SCIENCE
www.electrochemsci.org

The Fabrication of Multilayers of Conducting Polymers and Its High Capacitance Performance Electrode for Supercapacitor

Xiumei Ma[1,§], *Danhua Zhu*[1,§], *Daize Mo*[1], *Jian Hou*[2], *Jingkun Xu*[1,*], *Weiqiang Zhou* [1,*]

[1] Jiangxi Key Laboratory of Organic Chemistry, Jiangxi Science and Technology Normal University, Nanchang 330013
[2] State key laboratory for marine corrosion and protection, Luoyang ship material research institute, Qingdao, 266101, China
[*]E-mail: xujingkun@tsinghua.org.cn
§ Xiumei Ma and Weiqiang Zhou, These authors contributed equally to this work.

Received: 24 June 2015 / *Accepted:* 20 July 2015 / *Published:* 26 August 2015

In this work, 3-layered PEDOT/PBEDOT-BT/PEDOT electrode processed by alternated layers of poly(3,4-ethylenedioxythiophene) (PEDOT) and poly[5,5'-bis(2,3-dihydrothieno[3,4-*b*][1,4]dioxin-5-yl)-2,2'-bithiophene](PBEDOT-BT) were prepared by electrochemical layer-by-layer deposition. The electrochemical and structural properties and the capacitive properties of it were investigated through the methods of scanning electron microscopy, atomic force microscopy, galvanostatical charge-discharge, cyclic voltammetry and electrochemical impedance spectroscopy techniques. In all cases, the capacitive properties of 3-layered PEDOT/PBEDOT-BT/PEDOT systems were better than those of individual conducting polymers (PEDOT or PBEDOT-BT), which may be caused by the synergistic effects at the interfaces between consecutive layers and the higher porosity of the 3-layered materials. Furthermore, 3-layered PEDOT/PBEDOT-BT/PEDOT electrode has been used to fabricate a symmetric supercapacitor (assembled by two identical electrodes), which showed a high specific capacitance (97 F g^{-1}) and an excellent specific energy (260 Wh kg^{-1}).

Keywords: Supercapacitors, Poly(3,4-ethylenedioxythiophene), Conducting polymers, Multilayer, Electrodeposition

1. INTRODUCTION

Supercapacitors, also called electrochemical capacitors, has attracted widespread attention in recent years because of the combined distinguish advantages of its high power density, fast charge and discharge rate, long cycle life, *etc* [1-5]. In general, there are mainly three supercapacitors electrode

materials, namely carbon materials, conducting polymers (ECPs), transition metal oxides and hydroxides, and their compounds [6].

ECPs, such as polyaniline (PANI), polypyrrole (PPy), polythiophene (PTh) and their derivatives [7], as promising electroactive materials for supercapacitor, have been extensively studied by many researchers. Among them, poly (3,4-ethylenedioxythiophene) (PEDOT) was an excellent ECPs electrode material because of chemical stability and good thermal performance, high electrical conductivity (up to 550 S cm^{-1}), lower toxicity, fast electrochemical switching, and especially wider potential window (> 2.0 V) [8-11]. However, PEDOT presented a moderate value of theoretical specific capacitance (210 F g^{-1}) compared to PANI (750 F g^{-1}) and PPy (620 F g^{-1}) [9] because of its relatively high molar mass. In order to reach their theoretical specific capacitance, the ECPs composites with nanostructure carbon materials or metal oxides, novel dopant schemes, microstructure modification of ECPs, and developing asymmetric devices were developed in the past research [12-16].

On the other hand, electrochemical layer-by-layer (LbL) technique used to prepare bilayers or multilayer made of two or more different ECPs through electrodeposition techiniques was developed. In this methodology, individual anodic polymerization processes was used to prepare films formed by different layers and as-prepared ECPs/ECPs composite shown some interesting properties when compared with the individual ECPs homopolymers, such as highly porous structure, high specific capacitance, and good cycleability [17-20]. Xu et al [21] prepared PEDOT/PPy composite electrode by electropolymerization PEDOT on the surface of PPy, which shown much higher specific capacitance (> 200 F g^{-1}) than the values of either pure PEDOT or PPy electrode due to the synergic effect of PEDOT and PPy. Moreover, David Aradilla and co-workers [19] recently reported a multilayered conducting systems that alternate PEDOT and poly(N-methylpyrrole) (PNMPy), the multilayer showed better electrochemical performance and a excellent ability to store charge than each of the two individual ECPs. This improvement was attributed to both the synergistic effects at the interfaces between consecutive layers and the higher porosity of the prepared multilayered materials. Later, they also fabricated symmetric supercapacitors that based on three-layered ml-PEDOT/PNMPy supercapacitor and the specific capacitance of this supercapacitor not only significantly higher than that of the PEDOT but also similar to the advanced ultracapacitors reported in the literature [18]. In addtion, the researchers also perpared other multisystems and bilayers, include ml-PEDOT/PPy [17], ml-PEDOT/poly(N-cyanoethylpyrrole) (PNCPy) [19], PPy/PNMPy [22], and PPy/PPy [23-24]. Poly[5,5'-bis(2,3-dihydrothieno[3,4-*b*][1,4]dioxin-5-yl)-2,2'-bithiophene](PBEDOT-BT) (Scheme 1) [25], a PEDOT based copolymers, showed higher specific capacitance values (171 F g^{-1} at 1 A g^{-1}) than PEDOT and excellent stability. Based on the above results, we fabricated multilayer systems based on PEDOT and PBEDOT-BT to acheieve better capacitance performances of the corresponding supercapacitor electrodes.

Herein, we take the electrochemical LbL technique to assemble 3-layered PEDOT/PBEDOT-BT/PEDOT electrode made of alternated PEDOT and PBEDOT-BT films (i.e. PEDOT/PBEDOT-BT/PEDOT films in which both the internal and external layers are PEDOT while the intermediate layer is PBEDOT-BT) (Scheme 2) (for comparison, the individual PEDOT electrodes were also perpared and measured). The capacitance properties of fabricated 3-layered PEDOT/PBEDOT-

BT/PEDOT electrodes were tested by galvanostatical charge-discharge, cyclic voltammetry (CV) and electrochemical impedance spectroscopy (EIS) techniques. In addition, the morphology of the electrodes were also minutely studied by using scanning electron microscopy (SEM), cross-section SEM micrographs, and atomic force microscopy (AFM).

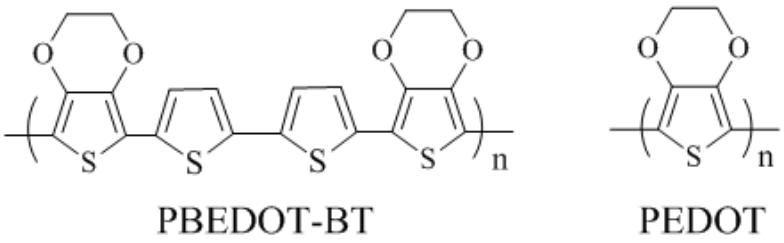

Scheme 1. The structure of PBEDOT-BT and PEDOT.

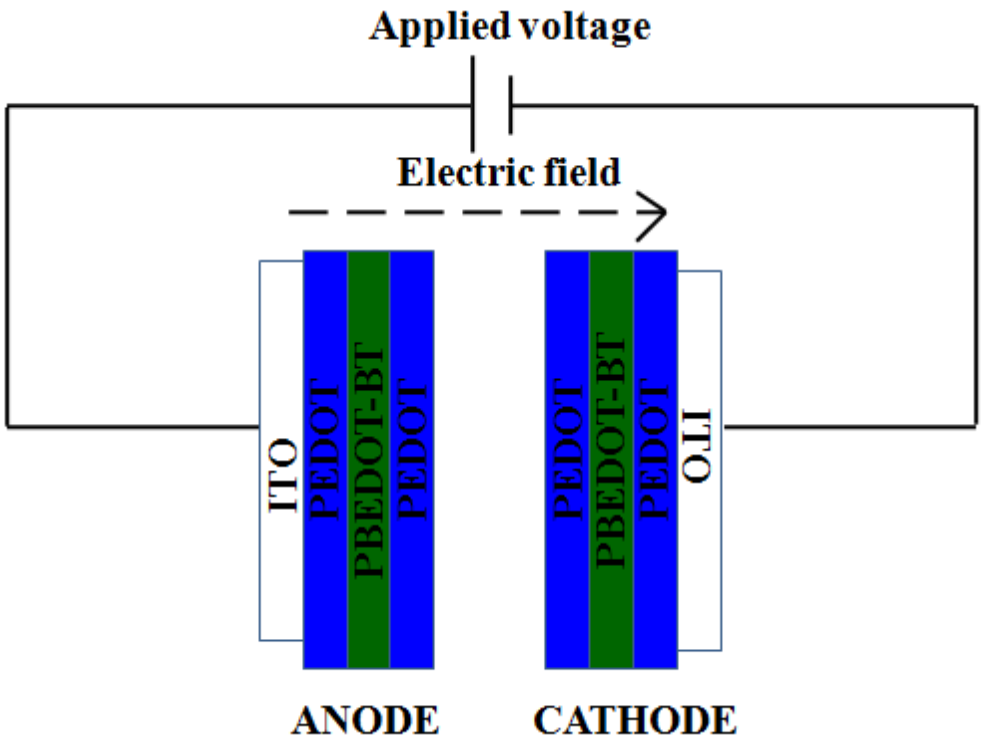

Scheme 2. Scheme of the supercapacitors assembled with two identical electrodes of 3-layered PEDOT/PBEDOT-BT/PEDOT deposited on indium tin oxide (ITO) films.

2. EXPERIMENTAL

2.1 Materials

BEDOT-BT was synthesized according to the previous reported method as described in literature [25]. 3,4-Ethylenedioxythiophene (EDOT) and tetrabutylammonium hexafluorophosphate

(Bu_4NPF_6) were purchased from Energy Chemical (Shanghai, China) and used as received. Acetonitrile (CH_3CN, > 99%, Beijing East Longshun Chemical Plant) and dichloromethane (CH_2Cl_2) was purified by distillation with calcium hydride under a nitrogen atmosphere before use.

2.2 Materials Characterization

The surface morphologies images and cross-section SEM micrographs of the polymers were attained on a JEOL JSM-6700F microscope operated at 5 kV. The AFM measurements were conducted on a NanoScope IIIa MultiMode in contact mode at room temperature under ambient conditions with commercially available etched silicon nitride probes. The root-mean-square roughness was tested by the statistical application of the Nanoscope software, which evaluates the average considering all the values recorded in the topographic image with exception of the maximum and the minimum.

2.3 The preparation of the polymer films

In this work, the potentiostatic method was employed to prepare polymer film at suitable electrode potential on indium tin oxide (ITO) substrate in a one-compartment cell with a CHI 660B potentiostat/galvanostat (Shanghai Chenhua Instrumental Co., Ltd. China). The electrolyte solution was 5 mL CH_3CN containing 10 mM m L^{-1} monomer and 0.1 M L^{-1} Bu_4NPF_6. PEDOT and PBEDOT-BT films were prepared at a constant potential of 1.4 V and 0.7 V *vs*. Ag/AgCl, respectively. The polymerization time used to produce individual PEDOT films was 30 s. The electrochemical LbL technique was used to prepare the 3-layered PEDOT/PBEDOT-BT/PEDOT films. The working electrode was immersed for a period of 10 s to prepare the each layer. The total polymerization time, 3 $\times$10 s = 30 s, was identical to that of individual PEDOT films. All the electrochemistry experiments were operated in a three electrode cell at room temperature. Indium tin oxide (ITO) and platinum wire (1.0 mm diameter) were used as the work electrode and the counter electrode, respectively. An Ag/AgCl electrode was used as the reference electrode. After polymerization, the working electrode was washed thoroughly with CH_2Cl_2 to remove any residue, and then dried under the air for further characterization.

2.4. Electrochemical Characterization

All the electrochemical measurements were measured using a CHI 660B electrochemical workstation in a conventional three-electrode system equipped with a as-prepared electrode, a platinum electrode and an Ag/AgCl electrode as the working electrode, counter electrode, and reference electrode, respectively. Before electrochemical measurements, O_2 was drived away of the solution by the inert gas N_2. The electrolyte was a 5 mL CH_3CN solution containing 0.1 M Bu_4NPF_6. The capacitive performances of the electrodes were investigated by cyclic voltammetry, galvanostatic charge-discharge techniques, and EIS measurements. EIS measurements of all the samples were

operated in the frequency range of 100 kHz to 0.01 Hz with an AC voltage amplitude of 5 mV, and an open circuit potential of 1.0 V (*vs* Ag/AgCl).

3. RESULTS AND DISCUSSION

3.1 Structure Characterization

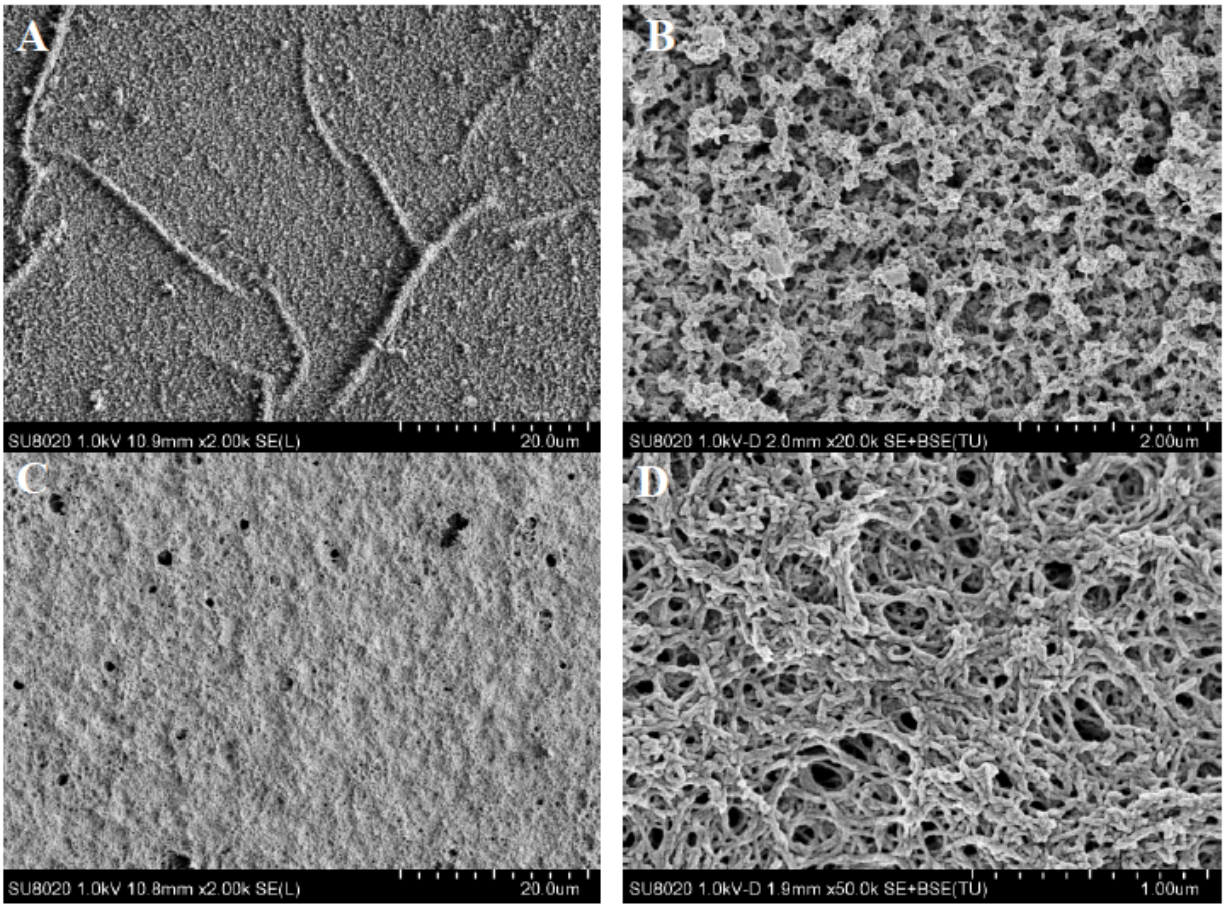

Figure 1. SEM images of PEDOT (A, B) and 3-layered PEDOT/PBEDOT-BT/PEDOT PBEDOT-BT-BO (C, D). Magnification: (A) and (C), 2000×, (B) and (D) 10,000×.

The capacitive performances of PEDOT and 3-layered PEDOT/PBEDOT-BT/PEDOT can be explained by the surface morphology of the polymer films. SEM images of PEDOT films (Figure 1) suggest that a heterogeneous and porous morphology was formed. However, a significant difference which is in accordance with the highest SC values observed in 3-layered PEDOT/PBEDOT-BT/PEDOT, that is PEDOT layers grown on the PBEDOT-BT layers of the multilayered films are nanowires structure and are more porous than PEDOT films which were directly electrodeposited on an ITO substrate. As a supercapacitor material, this porous nano-structure film shows advantages as follows: (1) the micro/nano-sized pores are beneficial for depolarization of the ion concentration and provide a high interfacial reaction area; (2) the porous network of 3-layered PEDOT/PBEDOT-

BT/PEDOT electrode creates efficient diffusion paths for electrolyte ions, which would significantly accelerate the intercalation of ions and enhance the utilization rate of electrode materials [26].

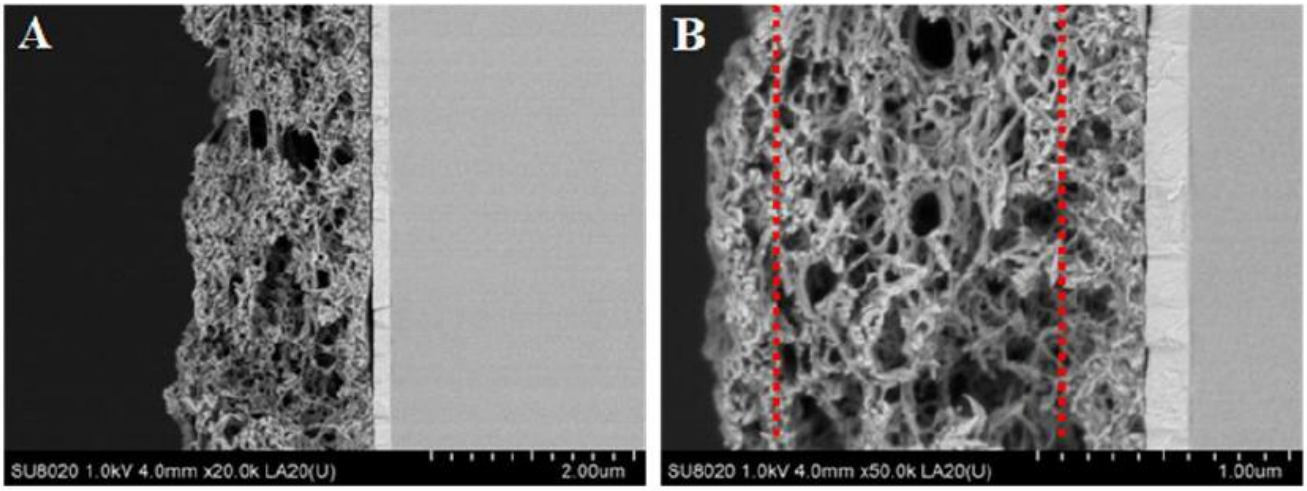

Figure 2. Cross-section SEM micrographs of the 3-layered PEDOT/PBEDOT-BT/PEDOT film. Magnification: (A) 20000×, (B) 50000×.

Figure 2 A&B presents the high resolution micrographs of the cross-section of a 3-layered PEDOT/PBEDOT-BT/PEDOT film, which allows the visual identification of alternated layers of PEDOT and PBEDOT-BT. The cross-section image of it also proves to be the porous structure of the 3-layered PEDOT/PBEDOT-BT/PEDOT electrode.

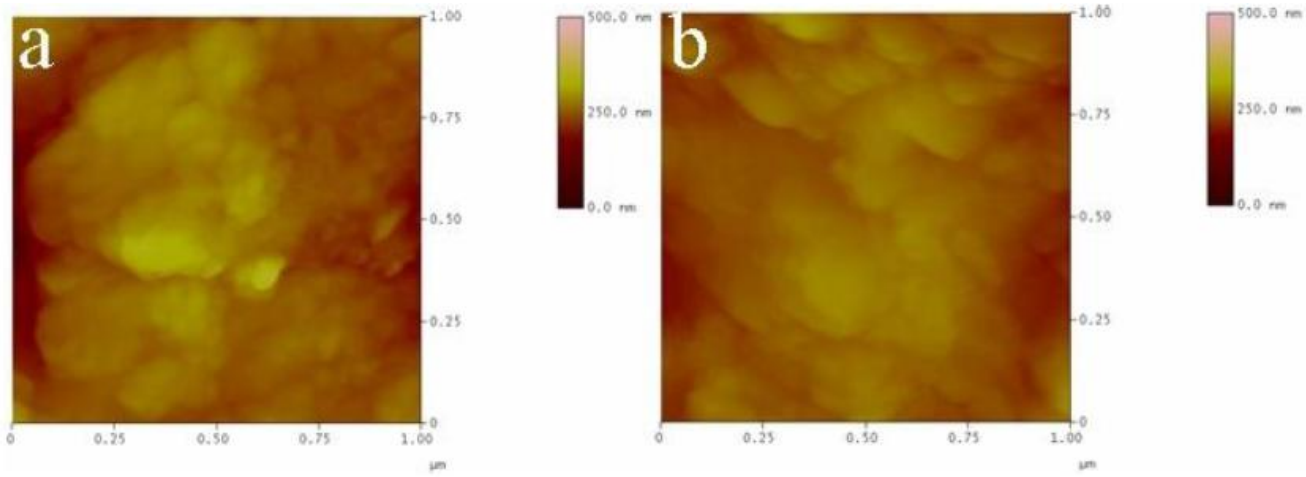

Figure 3. Height AFM images of 3-layered PEDOT/PBEDOT-BT/PEDOT (a) and PEDOT (b).

Figure 3 reveals a comparison of AFM height images of the PEDOT (Figure 3a) and 3-layerd PEDOT/PBEDOT-BT/PEDOT electrode (Figure 3b). The determined roughness by AFM images is 318.60 nm and 130.67 nm for PEDOT electrode and 3-layered PEDOT/PBEDOT-BT/PEDOT

electrode, respectively. These values confirm that the intermediate PBEDOT-BT layer increases the roughness of the external PEDOT layer. Above all, 3-layered PEDOT/PBEDOT-BT/PEDOT presents both increased and enlarged pores than PEDOT films, explaining the different SC values determined for the two such systems.

3.2 Capacitance performances of the electrodes

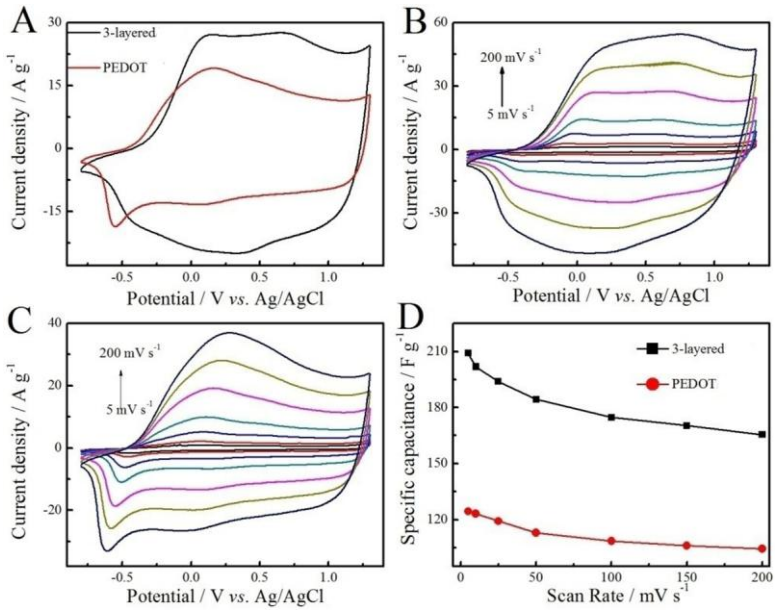

Figure 4. (A) Cyclic voltammograms of 3-layered PEDOT/PBEDOT-BT/PEDOT and PEDOT electrodes at scan rate of 100 mV s^{-1}; Cyclic voltammograms of 3-layered PEDOT/PBEDOT-BT/PEDOT (B) and PEDOT (C) electrodes in monomer-free CH_3CN-Bu_4NPF_6 (0.1 M) at potential scan rates of 200, 150, 100, 50, 25, 10, and 5 mV s^{-1}, and specific capacitance of the electrodes as a function of its scan rate (D).

Table 1. The specific capacitance of 3-layered PEDOT/PBEDOT-BT/PEDOT and PEDOT electrodes under different scan rate

Scan rate (mV s^{-1})	5	10	25	50	100	150	200
PEDOT/PBEDOT-BT/PEDOT (F g^{-1})	209	202	194	184	178	170	166
PEDOT (F g^{-1})	124	123	119	113	109	106	104

For the determination of the electrochemical capacitive properties of 3-layered PEDOT/PBEDOT-BT/PEDOT electrodes, CV tests in the range of -0.8-1.3 V at a scan rate of 5 to 100 mV s^{-1} were carried out in 0.1 M Bu_4NPF_6 (0.1 M)/CH_3CN electrolytes, which is shown in Figure 4. The shapes of the CV curves indicate the electric double-layer capacitance that mainly originates from pseudo-capacitance. The surrounding area of the CV curve loop of the 3-layered PEDOT/PBEDOT-BT/PEDOT electrode is clearly larger than that of PEDOT electrodes at the same scan rate (Figure

4A). The CV curve consisting of a couple of broad anodic and cathode peaks was very different from that of electric double layer capacitance whose CV curve is normally close to an ideal rectangular shape. This suggested that the charge capability of 3-layered PEDOT/PBEDOT-BT/PEDOT film is due to its ability to undergo electro-oxidation and electro-reduction [27]. The curves' shape only slightly changed even at the high scan rate of 200 mV s^{-1}, which resulted from the improved mass transportation within the electrode materials. With the scan rates increasing, gradually increasing current densities of the CV curves was observed and both the oxidation and the reduction peaks have a shift to more positive and negative potential, respectively, which was probably ascribed to the diffusion of PF_6^- ions. At low scan rates the PF_6^- ions diffuse more slowly, so the active materials can have a full reaction with PF_6^- ions and have a higher utilization ratio [28]. The peak current densities are in proportion to the potential scan rate, which indicates the reversible and not diffusion-limited electrochemical processes of the electrodes. The specific capacitances derived from CV tests can be obtained from the following Equation (1):

$$C_s = \frac{q_a + q_c}{2mv\Delta V}$$

In which C_s (F g^{-1}), q_a, q_c, v (V s^{-1}), m (g), and ΔV (V) are the specific capacitance, the sums of anodic and cathodic voltammetric charges on the anodic and cathodic scans, the scan rate, the mass of the active material and the potential range of CV, respectively.

The calculated specific capacitances according to the CV curves at scan rates of 5-200 mVs^{-1} are presented in Figure 4D. From the CV curves in Figure 4B, the specific capacitances of the 3-layered PEDOT/PBEDOT-BT/PEDOT electrodes are calculated to be 209, 202, 194, 184, 175, 170 and 166 F g^{-1} at scan rates of 5, 10, 25, 50,100, 150 and 200 mV s^{-1}. The specific capacitance of the 3-layered PEDOT/PBEDOT-BT/PEDOT electrode can reach 209 F g^{-1} and PEDOT electrode can reach 124 F g^{-1} at 5 mV s^{-1}. Even though the specific capacitance of the 3-layered PEDOT/PBEDOT-BT/PEDOT electrode decreases with the scan rate increasing, the specific capacitance still has an ideal value. The observed decrease can be explained based on the ion-exchange mechanism. It will take enough time for PF_6^- to transfer between the solution and the surface of the electrode material to allow intercalation/extraction into/out of the electrodes when charging/discharging. When at low scan rate, such as 5 mVs^{-1}, PF_6^- has enough time to transfer and there is much more charge transferred than that at a high scan rate; thus more charge can be stored, resulting in higher specific capacitance [29]. As stated above, the 3-layered PEDOT/PBEDOT-BT/PEDOT electrode in Bu_4NPF_6 (0.1 M)/CH_3CN electrolytes clearly has excellent electrochemical capacitive performance, even at a high scan rate.

Rate capability is a key factor to evaluate the power application of supercapacitor. The charge-discharge curves of the 3-layered PEDOT/PBEDOT-BT/PEDOT electrode and PEDOT electrode at current densities from 1 A g^{-1} to 15 A g^{-1} are shown in Figure 5A and Figure 5B. The long charging/discharging time indicates the 3-layered PEDOT/PBEDOT-BT/PEDOT electrode material might possess a good electrochemical capacitive performance and a good reversible redox reaction. The nonlinear charge-discharge curves confirmed the pseudocapacitance nature of the 3-layered PEDOT/PBEDOT-BT/PEDOT electrode, which was in agreement with the CV results. There was no visible ohmic loss (IR drop) at all current densities, indicating that the 3-layered PEDOT/PBEDOT-BT/PEDOT electrode had a small resistance.

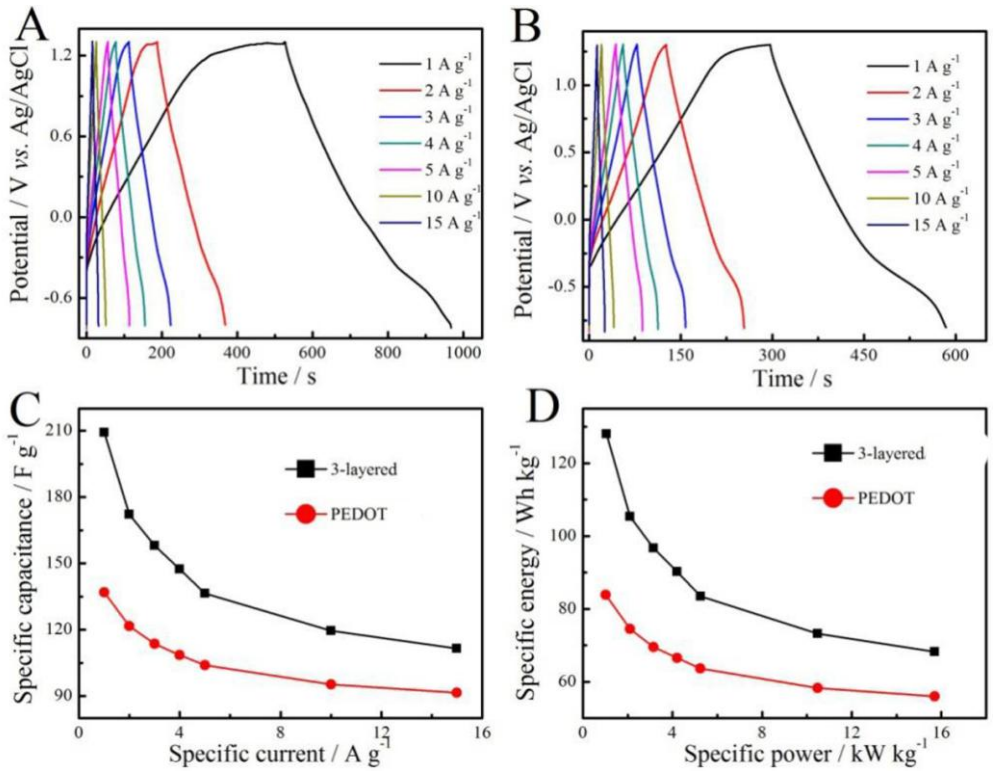

Figure 5. Galvanostatic charge/discharge curves of 3-layered PEDOT/PBEDOT-BT/PEDOT (A) and PEDOT (B) in CH_3CNsolution containing 0.1 M Bu_4NPF_6 at different current density; (C) Specific capacitance of the electrodes as a function of current density; (D) Specific power as a function of specific energy

Table 2. The specific capacitance of 3-layered PEDOT/PBEDOT-BT/PEDOT and PEDOT electrodes under different current densities

Specific current (A g^{-1})	1	2	3	4	5	10	15
PEDOT/PBEDOT-BT/PEDOT (F g^{-1})	209	172	158	147	136	120	111
PEDOT (F g^{-1})	136	122	114	109	104	95	91

The specific capacitance (C) obtained from galvanostatic charge/discharge method was calculated according to the equation as follows (4):

$$C = \frac{I\Delta t}{m\Delta V}$$

Where ΔV (V) represents the discharge potential range, I (A) stands for the constant charge or discharge current density, m (g) expresses the active material mass, and Δt (s) is the corresponding discharge time. The specific capacitances derived from the discharging curves at a current density range from 1 to 15 A g^{-1} are presented in Figure 5C. The specific capacitance of the 3-layered PEDOT/PBEDOT-BT/PEDOT electrode at a current density of 1 A g^{-1} is calculated to be 209 F g^{-1}. When at a high current density of 15 A g^{-1}, the obtained specific capacitance of the 3-layered PEDOT/PBEDOT-BT/PEDOT electrode reaches 111 F g^{-1}, which is still higher than that of PEDOT at

the same conditions. From these results, we can concluded that the specific capacitance of the 3-layered PEDOT/PBEDOT-BT/PEDOT electrode is significantly better than many other traditional conducting polymers, such as PTh (117 F g^{-1}) [30], PPy (186 F g^{-1}) [31], PANI (216 F g^{-1}) [32], and polyselenophene (PSe) (72.2 F g^{-1}) [33]. Such good rate capability in the 3-layered PEDOT/PBEDOT-BT/PEDOT electrode can be ascribed to the reduced diffusion path of ions and the highly accessible surface area for the porous nanowires structure.

Specific energy and specific power are also two significant parameters to evaluate the power application of supercapacitor. An excellent supercapacitor should provide high energy density and high specific capacitance at high charging-discharging rates (current densities). Specific energy (E in Wh kg^{-1}) and specific power (P in W kg^{-1}) derived from galvanostatic charge/discharge tests can be calculated from Equations (3) and (4), respectively:

$$E = \frac{1}{2} C \Delta V^2 \qquad (3)$$

$$P = \frac{E}{\Delta t} \qquad (4)$$

in which C (F g^{-1}), ΔV (V), and Δt (s) are the specific capacitance, the potential range of the charge/discharge, and discharge time, respectively. Figure 5D is the plots of estimates of specific energy and specific power for the 3-layered PEDOT/PBEDOT-BT/PEDOT electrode in the electrolyte. While the specific power increases as the current increased from 1 to 15 A g^{-1}, the specific energy decreases. The 3-layered PEDOT/PBEDOT-BT/PEDOT electrode shows a high specific energy and specific power. The specific energy of the 3-layered PEDOT/PBEDOT-BT/PEDOT electrode decreases from 36 to 23 Wh kg^{-1}, while the specific power increases from 115 to 1160 kW kg^{-1}. For comparison, the PEDOT electrode shows a small specific energy (from 17 to 10 Wh kg^{-1}) and corresponding specific power (from 119 to 1313 kW kg^{-1}) values.

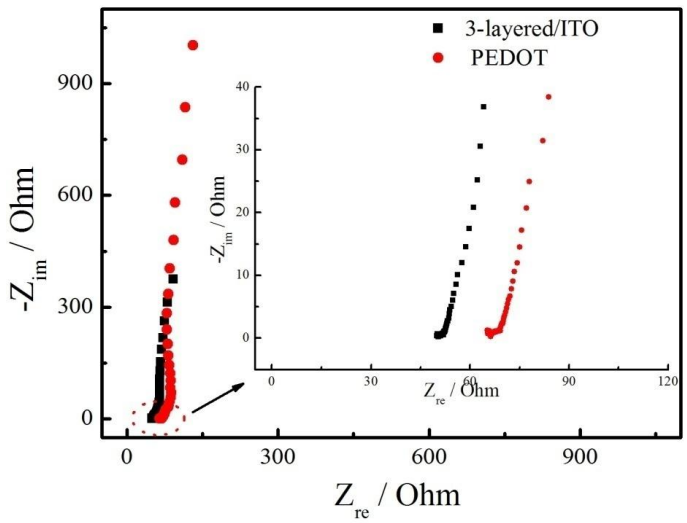

Figure 6. The impedance spectra of 3-layered PEDOT/PBEDOT-BT/PEDOT and PEDOT electrodes in CH_3CN-Bu_4NPF_6 solution at 1.0 V.

These results indicated the high specific power and specific density of the 3-layered PEDOT/PBEDOT-BT/PEDOT electrode, and this electrode may have potential application in the field of supercapacitor.

EIS is a good method used to evaluate the electrochemical performance of the electrodes. Figure 6 shows the Nyquist plots of the EIS spectra of the electrodes. The two impedance curves show a semicircle in the high frequency region and a nearly vertical straight line in the low frequency region, suggesting that the electrode process is dominated by charge transfer and charge diffusion, respectively [34]. The bulk solution resistance R_s, which can be used to evaluate the resistance associated with the transports within the porous structures and charge-transfer resistance R_{ct} was obtained from the Nyquist plots, where the high frequency semicircle intercepts the real axis at R_s and (R_s+R_{ct}). The solution resistance R_s of 3-layerer/ITO PEDOT/PBEDOT-BT/PEDOT electrode and PEDOT electrode was tested to be 50.0 Ω and 65.3 Ω, respectively. These low resistances may result from the porosity of the two systems, which benefit the access and escape of dopant anions into the inner polymer. In addition, the higher porosity of 3-layered PEDOT/PBEDOT-BT/PEDOT electrode is consistent with its lower resistance. The charge-transfer resistance R_{ct} was evaluated to be 2.5 Ω for 3-layer/ITO PEDOT/PBEDOT-BT/PEDOT electrode and 4.6 Ω for PEDOT, respectively. These low values should result from the porous structure of the two materials, which increases the kinetic of electron transfer through redox processes. As R_{ct}, which is also called Faraday resistance, is a limiting factor for the specific power and the low Faraday resistance would lead to high specific power. The data from EIS spectra clearly demonstrate the 3-layered PEDOT/PBEDOT-BT/PEDOT electrode has slightly better capacitance behavior compared to PEDOT electrode.

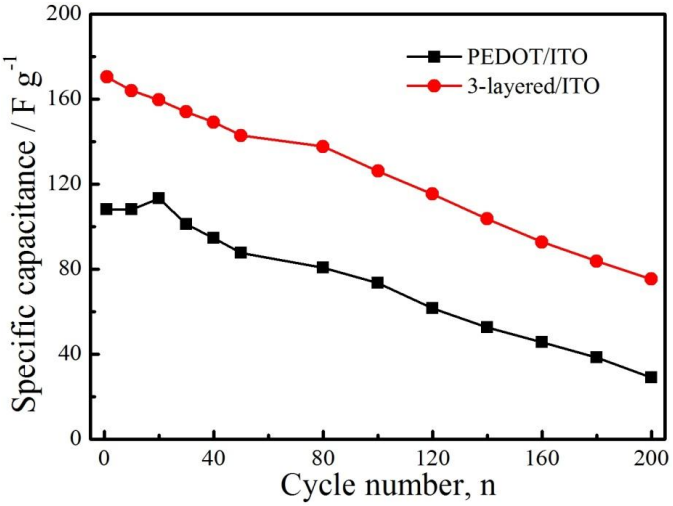

Figure 7. Cycle life of 3-layered PEDOT/PBEDOT-BT/PEDOT and PEDOT electrode in CH_3CN-Bu_4NPF_6 solution.

Specific capacitance retention is another important parameter for a good electrode materials [35,36]. An excellent supercapacitor should work steadily, which request the specific capacitance of the electrode materials change as little as possible. Specific capacitance as a function of cycling

number of the 3-layered PEDOT/PBEDOT-BT/PEDOT materials in Bu_4NPF_6 (0.1 M)/CH_3CN electrolytes are shown in Figure 7. The stability of the 3-layered PEDOT/PBEDOT-BT/PEDOT electrode was not very competitive. The 3-layered PEDOT/PBEDOT-BT/PEDOT electrode shows relative poor specific capacitance retention at scan rate of 150 mV s^{-1}. After the initial 200 cycles, the 3-layered PEDOT/PBEDOT-BT/PEDOT electrode maintains 44.2% retention (28% for PEDOT electrodes) of its initial value. The obvious degradation in the specific capacitance of the 3-layered PEDOT/PBEDOT-BT/PEDOT electrode possibly results from the broad work potential window of the electrodes (The electrochemical stability of each ECP is strictly effected by its working potential range and/or polymer degradation caused by overoxidation [37]).

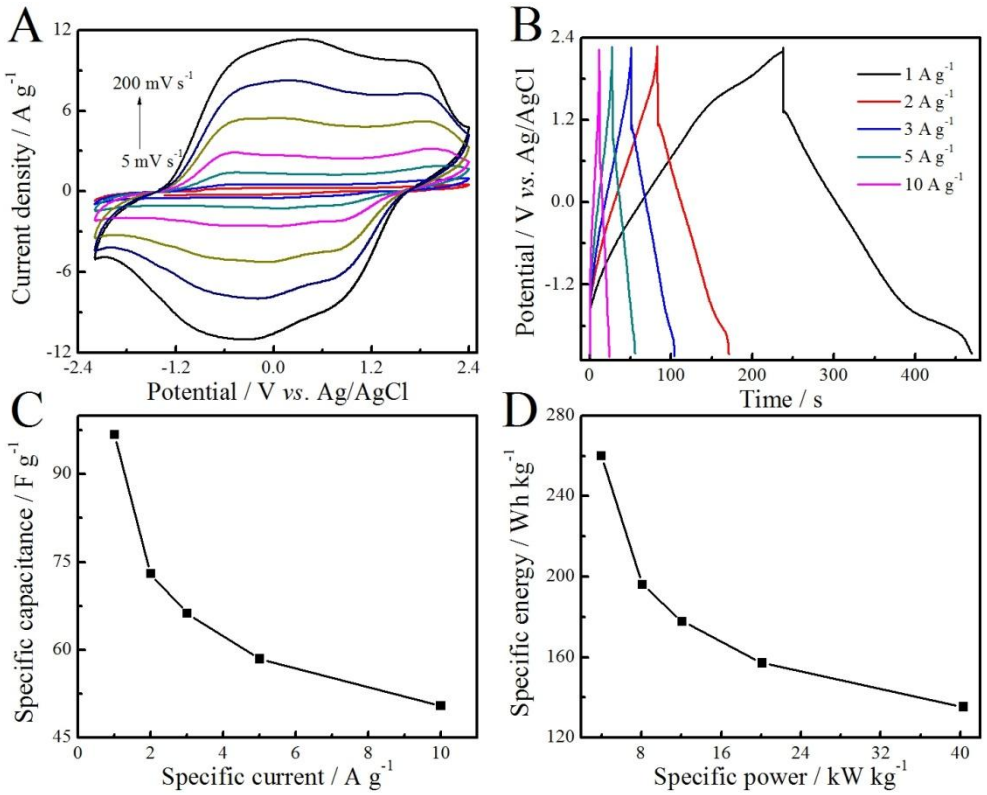

Figure 8. (A) CV curves and (B) galvanostatic charge/discharge curves of the self-assembled supercapacitor based on two identical 3-layered PEDOT/PBEDOT-BT/PEDOT electrodes, (C) Specific capacitance as a function of specific current of the symmetric supercapacitor, (D) Specific energy as a function of specific power.

To further evaluate the merit of the electrodes, a symmetric capacitor was assembled employing two identical 3-layered PEDOT/PBEDOT-BT/PEDOT electrodes both as the positive electrode and the negative electrode. Figure 8A presents the CV curves of the 3-layered PEDOT/PBEDOT-BT/PEDOT supercapacitor with various scan rates. The relatively asymmetric responses upon charging and discharging suggested that an irreversible reaction happened in this voltage range. Two quasi-linear voltage-time responses in the potential region investigated were observed, however, the charge curve was not symmetric to its corresponding discharge counterpart for

the cell. The SC calculated for the assembled supercapacitor with two identical 3-layered PEDOT/PBEDOT-BT/PEDOT electrodes (97 F g^{-1}) is significantly higher (~123%) than that obtained for the supercapacitor based on two identical PEDOT electrodes. the SC values obtained for 3-layered PEDOT/PBEDOT-BT/PEDOT supercapacitor is only ~9% lower than those measured for chemically modified graphene ultracapacitors (~99 F/g) under similar experimental conditions [38].

4. CONCLUSIONS

In summary, a facile LbL electrodeposition technique was employed to fabricate porous 3-layered PEDOT/PBEDOT-BT/PEDOT electrode, and the potential applications in supercapacitors of the prepared electrode was explored in detail. The 3-layered PEDOT/PBEDOT-BT/PEDOT electrode exhibits higher specific capacitances with 209 F g^{-1} at 1 A g^{-1} and better cyclic ability. The outstanding performance comes from both the higher porosity and the synergistic effects at the interfaces between consecutive layers of the 3-layered film. A symmetric supercapacitor (SC) based on it shown a relatively high specific capacitance (97 F g^{-1}) and a high specific energy value of 260 Wh kg^{-1}. Therefore, the novel 3-layerd PEDOT/PBEDOT-BT/PEDOT is expected to be a promising electrode material for supercapacitors.

ACKNOWLEDGEMENTS
This work was supported by the Jiangxi Provincial Department of Education for postgraduate (YC2014-S435), National Natural Science Foundation of China (grant number: 51463008), Natural Science Foundation of Jiangxi Province (grant number: 20142BAB216029)

References

1. L.L. Zhang, X.S. Zhao, *Chem. Soc. Rev*., 38 (2009) 2520-2531.
2. P. Simon, Y. Gogotsi, *Nat. Mater.*, 7(2008) 845-854.
3. J.R. Miller, P. Simon, *Science*, 321 (2008) 651-652
4. A.S. Adekunle, B.O. Agboola, K.I. Ozoemena, E.E. Ebenso, J.A.O. Oyekunle, O.S. Oluwatobi, J.N. Lekitima, *Int. J. Electrochem. Sci.*, 10 (2015) 3414-3430
5. K.J. Sun, H.P. Wang, H. Peng, Y.J. Wu, G.F. Ma, Z.Q. Lei, *Int. J. Electrochem. Sci.*, 10 (2015) 2000-2013
6. Y. Zhang, H. Feng, X.B. Wu, L.Z. Wang, A.Q. Zhang, T.C. Xia, H.C. Dong, X.F. Li, L.S. Zhang, *Int. J. Hydrogen. Energ*., 34 (2009) 4889-4899.
7. C. Peng, S.W. Zhang, D. Jewell, G.Z. Chen, *Prog. Nat. Sci*., 18 (2008)777-788.
8. W.K. Li, J. Chen, J.J. Zhao, J.R. Zhang, J.J. Zhu, *Mater Lett.*, 59 (2005) 800-803.
9. K. Lota, V. Khomenko, E. Frackowiak, *J Phys Chem Solids*., 65(2004)295-301.
10. A. Czardybon, M. Lapkowski, *Synth. Met*., 119 (2001) 161-162.
11. B.E. Conway, Conway in Electrochemical Supercapacitors, Kluwer, New York, 1999.
12. G.P. Pandey, A.C. Rastogi, C.R. Westgate, *J. Power. Sources*, 245 (2014)857-865.
13. B. Babakhani, D.G. Ivey, *Electrochim. Acta*., 55 (2010) 4014-4024.
14. L. Li, D.C. Loveday, D.S.K. Mudigonda, J.P. Ferraris, *J. Electrochem. Soc*., 149 (2002) A1201.
15. J. Tanguy, M. Slama, M. Hoclet, J.L. Baudouin, *Synth. Met*., 28 (1989) 145-150.

16. M. Wilamowska, A. Lisowska-Oleksiak, *J. Power. Sources*, 194 (2009) 112-117.
17. D. Aradilla, M. M. Pérez-Madrigal, F. Estrany, D. Azambuja, J. I. Iribarren, C. Alemán, *Org. Electron*., 14 (2013) 1483-1495.
18. D. Aradilla, F. Estrany, C. Aleman, *J. Phys. Chem. C*., 115 (2011) 8430-8438.
19. D. Aradilla, F. Estrany, R. Oliver, C. Alemán, *Eur. Polym. J.*, 46 (2010) 2222-2228.
20. F. Estrany, D. Aradilla, R. Oliver, E. Armelin, C. Alema, Eur. Polym. J., 44 (2008) 1323-1330.
21. J.Wang, Y. L. Xu, X.Chen, X.F. Du, *J. Power. Sources*, 163 (2007) 1120-1125.
22. A.Wodja., K. Maksymiuk, *J. Electroanal. Chem*., 424 (1997) 93-99.
23. A. Kepas., M. Grzeszczuk, *J. Electroanal. Chem*., 582 (2005) 209-220.
24. M. Grzeszczuk, J. Kalenik, A. Kepas-Suwaran, *J Electroanal Chem*., 626 (2009) 47-58.
25. D.Z. Mo, W.Q. Zhou, X.M. Ma, J.K. Xu, D.H. Zhu, B.Y. Lu, *Electrochim. Acta*, 132 (2014) 67-74.
26. X.M. Ma, W.Q. Zhou, D.Z. Mo, Z.P. Wang, J.K. Xu, *Synth. Met*., 203 (2015) 98-106.
27. D.Z. Mo, W.Q. Zhou, X.M. Ma, J.K. Xu, *Electrochim. Acta*, 155 (2015) 29-37.
28. Y.L. Xiao, Y. Lei, B.Z. Zheng, L. Gu, Y.Y. Wang, D. Xiao, *RSC Adv*., 5 (2015) 21604-21613.
29. H. Pang, C.Z. Wei, Y.H. Ma, S.S. Zhao, G.C. Li, J.S. Zhang, J. Chen, S.J. Li, *Chem. Plus. Chem*., 78 (2013) 546-553.
30. B. Senthilkumar, P. Thenamirtham, R.K. Selvan, *Appl. Surf. Sci*., 257 (2011) 9063-9067.
31. J. Wang, Y.L. Xu, X. Chen, X.F. Sun, *Compos. Sci. Technol*., 67 (2007) 2981-2985.
32. Y.E. Miao, W. Fan, D. Chen, T.X. Liu, ACS Appl. Mater. Interfaces 5 (2013) 4423-4428.
33. J.W. Park, S.J. Park, O.S. Kwon, C. Le, J. Jang, *Chem. Mater*., 26 (2014) 2354-2360.
34. N. Li, D. Shan, H. Xue, *Eur. Polym. J.*, 43 (2007) 2532-2539.
35. Y. Xiao, C. Long, M.T. Zheng, H.W. Dong, B.F. Lei, H.R. Zhang, Y.L. Liu, *Chinese Chem. Lett.*, 25 (2014) 865-868.
36. M.J. Shi, S.Z. Kou, B.S Shen, J.W. Lang, Z. Yang, X.B. Yan, *Chinese Chem. Lett.*, 25 (2014) 859–864.
37. T. Kobayashi, H.Yoneyamal, H. Tamura, *J. Electroanal. Chem*., 177 (1984) 281-291.
38. M.D. Stoller, S. Park, Y. Zhu, J. Na, R.S. Ruoff, *Nano. Lett*., 8 (2008) 3498-3502.